ChemComm

Photoinduced Peeling of Molecular Crystals

Journal:	*ChemComm*
Manuscript ID	CC-COM-12-2018-010051.R1
Article Type:	Communication

COMMUNICATION

Photoinduced Peeling of Molecular Crystals

Fei Tong[a], Maram Al-Haidar[b], Lingyan Zhu[a], Rabih O. Al-Kaysi[b]*, Christopher J. Bardeen[a]*

Received 00th January 20xx,
Accepted 00th January 20xx

DOI: 10.1039/x0xx00000x

Block-like microcrystals composed of *cis*-dimethyl-2(3-(anthracen-9-yl)allylidene)malonate are grown from aqueous surfactant solutions. A pulse of 405 nm light converts a fraction of molecules to the *trans* isomer, creating an amorphous mixed layer that peels off the parent crystal. This photoinduced delamination can be repeated multiple times on the same block.

Photomechanical materials transform light directly into mechanical work.[1-3] While polymer-based materials that incorporate photochromic molecules have received much attention[4-6], molecular crystals composed solely of photochromic molecules can also execute a variety of motions under light exposure.[7-19] In order to observe shape changes of intact crystals, it is often necessary that at least one dimension is on the order of microns or less. In larger crystals, the build-up of internal strain due to the simultaneous presence of both reactant and product domains can lead to fracture and loss of crystal integrity.[20-22] Naumov and others have shown that release of kinetic energy during the fracture process can propel microcrystals over large distances (the photosalient phenomenon), but this fracturing tends to be difficult to control.[23-25] If a crystal could split apart in a controlled, reproducible way, photoinduced fracture might become a feature that could be harnessed. Such a material might have practical applications, ranging from controllable adhesion to mechanical switching to renewable surfaces.

Our goal in this work was to develop a molecular crystal material that can fragment in a controlled way under light irradiation. As mentioned above, the internal strain associated with a crystal-to-crystal photochemical reaction tends to lead to either crystal deformation or to fracture. A gentler approach is to use a solid-state photochemical reaction that generates an amorphous product phase. Ideally, the irregular molecular packing in the product would be incommensurate with the parent crystal, leading to phase separation into a layer that is soft enough to deform and detach without additional fracturing. As our photomechanical active element, we chose *cis*-dimethyl-2(3-(anthracen-9-yl)allylidene)malonate (*cis*-**DMAAM**), a divinyl anthracene derivative that can undergo a *cis*-to-*trans* photoisomerization reaction in both solution and crystal form (Scheme 1 and Figure S1, ESI). Both the *cis* and *trans* isomerization reactions result in an amorphous mixture that causes nanowires composed **DMAAM** to bend and coil.[26]

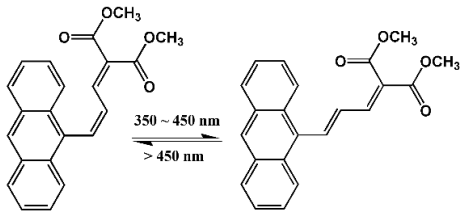

Scheme 1. Photoisomerization of the **DMAAM** molecule between *cis* and *trans* conformations.

Identification of a photochemical reaction is the first step. In order to clearly observe the physical separation of reactant and product regions, the second step is to prepare the appropriate crystal shape. This is because fracture and slip events tend to occur preferentially along specific crystal planes.[27-29] To design a molecular crystal system that undergoes a well-defined fragmentation, we must find crystal growth conditions that control faceting. Several groups have shown that varying parameters like concentration, temperature, and surfactant can lead to the growth of crystals with different shapes and faceting in aqueous solution.[30-38] In this Communication, we adapt this approach in order to grow block-shaped microcrystals composed of *cis*-**DMAAM**. We characterize the structure and dynamics of these crystals using a variety of experimental techniques to demonstrate that controlled fragmentation (or peeling) can indeed be accomplished using solid-state photochemical reactions.

[a] *Department of Chemistry, University of California, Riverside, 501 Big Springs Road, Riverside, CA 92521 (USA).Email: christopher.bardeen@ucr.edu*
[b] *College of Science and Health Professions-3124, King Saud bin Abdulaziz University for Health Sciences, and King Abdullah International Medical Research Center, Ministry of National Guard Health Affairs, Riyadh 11426, (Kingdom of Saudi Arabia). Email: rabihalkaysi@gmail.com*
Electronic Supplementary Information (ESI) available: [details of any supplementary information available should be included here]. See DOI: 10.1039/x0xx00000x

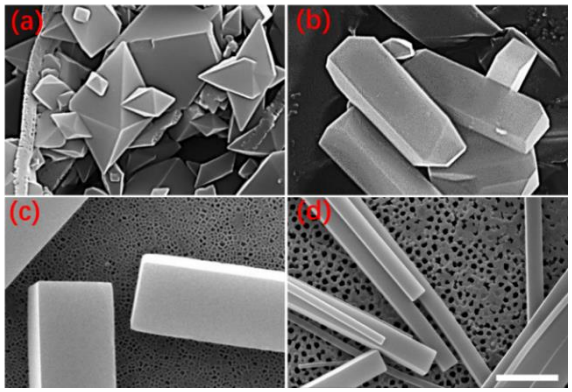

Figure 1. SEM images of different crystal shapes produced using various concentrations of 1-dodecanol with [SDS] = 0.02 M. (a) [1-dodecanol] = 0 M, (b) 0.0009 M, (c) 0.0022 M and (d) 0.0066 M. Scale bar = 4 μm.

Large plate-like *cis*-**DMAAM** crystals, suitable for single crystal structure determination, can be grown by slow ethanol/water solvent evaporation. In order to obtain different shapes, we use a seeded growth procedure in an aqueous solution containing a mixture of sodium dodecyl sulfate (SDS) and 1-dodecanol. The solution is maintained at a temperature between 40-42 °C to keep the 1-dodecanol dissolved and prevent it from co-crystalizing with SDS. [39] Varying the concentration of 1-dodecanol has a dramatic effect on the microcrystal shape. In Figure 1 and Figures S2-5, ESI, we show a series of SEM images of *cis*-**DMAAM** microcrystals grown at various 1-dodecanol concentrations with [SDS] = 0.02 M. For [1-dodecanol] = 0.0 M, we obtain octahedral crystals. As [1-dodecanol] is increased, new crystal facets appear that form a rectangular body capped by pyramidal ends. These octahedral crystals gradually evolve into well-defined rectangular block crystals with increasing length-to-width ratios for the highest 1-dodecanol concentrations.

Interestingly, the resulting suspensions of microblocks have reasonably narrow size distributions. This can be seen from the optical microscopy images of the blocks in Figure 2a and b, as well as the histograms of the block length and width distributions in Figure 2b-c and Figure S6, ESI. It is possible that the initial nucleation events are followed by gradual growth and exchange of molecules between crystals, facilitated by the presence of the surfactant, which contributes to the narrow size distributions. The ultimate width and length of the blocks can be tuned somewhat by varying the values of [SDS], [1-dodecanol], and the agitation process, but the transformation from octahedral to block prism is robust as long as [1-dodecanol] > 0.001 M. A preliminary survey of other surfactant conditions suggests that the SDS/1-dodecanol combination is the most effective for growing block-shaped crystals. Replacing 1-dodecanol with longer chain alcohols like 1-hexadecanol, 1-octadecanol, or 1H, 1H, 2H, 2H-perfluoro-1-dodecanol results in randomly sized octahedrons. The solubility of these long-chain alcohols in SDS is considerably lower than that of 1-dodecanol. Likewise, the use of other surfactants such as cetyl trimethyl ammonium bromide (CTAB), Tween-80, or Pluronic F-127 yields small, irregularly shaped *cis*-**DMAAM** microcrystals. In all these surfactants, 1-dodecanol was sparingly soluble and could not be

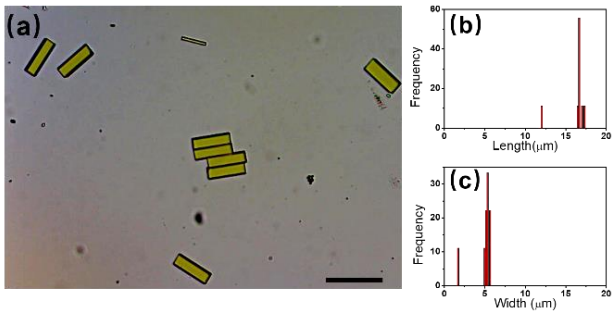

Figure 2. (a) Optical microscope images of *cis*-**DMAAM** microcrystals prepared using 25 μL of seed solution with [SDS] = 0.02 M and [1-dodecanol] = 0.0022 M. Scale bar = 25 μm. (b) and (c) histograms of length and width distributions of *cis*-**DMAAM** microcrystals.

effectively co-dissolved. It may be possible to find other surfactant/alcohol combinations that promote the growth of different crystal habits, but such a survey is beyond the scope of this Communication.

The ability of surfactants to modify crystal shape and faceting has been observed for many different organic molecules.[30-38] While a detailed mechanistic understanding of this phenomenon is still lacking, it is likely that stabilization of different crystal faces by the surfactants plays a key role.[40] We use PXRD to identify the crystal planes along the flat sides of the block crystals, as described in the ESI. By careful drying, we can make samples in which the blocks lie horizontal along their long axis on the substrate. A PXRD measurement, shown in Figure 3a, can then be used to determine which Miller planes lie parallel to the substrate. The assignment of the Miller indices is done by matching the observed peaks with those from a PXRD pattern calculated from the single crystal structure (Figure 3b). The prominent peaks due to parallel (110), (220) and (330) Miller planes indicate a preferred orientation with the (110) plane aligned parallel to the long axis of the blocks. This arrangement of *cis*-**DMAAM** molecules is shown in Figure 3c. Note that these assignments assume that the microblock crystals are the same polymorph as those used for x-ray structure determination. We attempted to confirm this by grinding the microblocks into a powder, but this procedure results in the loss of all PXRD peaks, presumably due to amorphization.

After preparing assemblies of microcrystals with well-defined sizes and shapes, we can assess their photomechanical response.

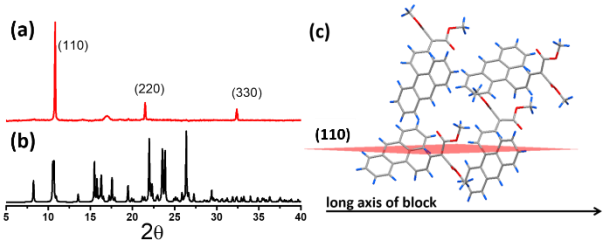

Figure 3. (a) PXRD patterns of *cis*-**DMAAM** microcrystals laying horizontally to surface. (b) Calculated PXRD patterns of *cis*-**DMAAM** molecule from single crystal showing corresponding peaks. (c) Molecular arrangement of *cis*-**DMAAM** microblock crystals along their long axis, which runs parallel to the (110) Miller plane.

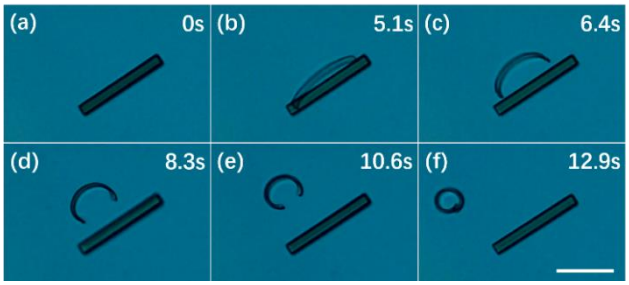

Figure 4. Sequence of optical microscopy images of a *cis*-**DMAAM** microcrystal undergoing photoinduced peeling process after a 1 s exposure to 405 nm light. Scale bar is 5 μm. The numbers upright indicate the time after light irradiation.

When the octahedral crystals in Figure 1a are exposed to 405 nm light, there is some evidence of surface roughening and blister formation, but complete fracture and separation of fragments are not observed. Even though NMR analysis confirms that these crystals are undergoing *cis*→*trans* photoisomerization, their large size prevents the curling seen in the nanowires (Figure S7 and S8, ESI). In addition, the octahedral habit contains exposed crystal facets that are not oriented correctly to facilitate laminar layer separation. But when block-like crystals are grown, we see a novel response: photoinduced peeling of surface layers. Figure 4 illustrates a sequence of events: the crystal block is first exposed to a flash of 405 nm light from a 100 W medium pressure Hg lamp (100 mW/cm^2) for a duration of 1 s. After this exposure, a longitudinal section begins to delaminate and curl against the parent crystal, finally detaching from the main block after 10-20 s. Videos of this process have been included in Movies S1 and S2, ESI. This process can be repeated multiple times until the original block disappears completely. Delamination can happen from all sides of the microblock with equal rates, as seen from randomly dispersed microblocks in Movie S2, ESI. The 405 nm irradiation wavelength was chosen because of the strong absorption of the *cis* isomer at this wavelength. Other wavelengths (365 nm, 462 nm) induce peeling as well, albeit at slower rates. Heating by the light source probably plays a negligible role since no peeling was observed in the absence of light at temperatures up to 60°C and no enhancement of the light-induced peeling was observed for temperatures up to 40°C (Figure S9, ESI).

The presence of SDS in solution is necessary for the peels to fully detach from the parent crystal. When the SDS is removed after centrifugation and resuspension of the microblocks in pure water, surface distortions and partial delamination are observed but not clean detachment. The photomechanical behavior also depends on the crystal dimensions. Microblocks with cross sections < 700 nm tend to spontaneously coil instead of peel after a 1 s light pulse (Movie S3, ESI). Large (100 μm thick) microblocks develop cracks but do not deform or peel (Figure S6, ESI). In some cases the thin microblocks, grown from high concentrations of 1-dodecanol, fuse together to form tetra and hexapods that can be triggered with UV light to spontaneously close in a clamping action (Movies S4 and S5, ESI). This type of structure could be used to develop functional photomechanical devices.

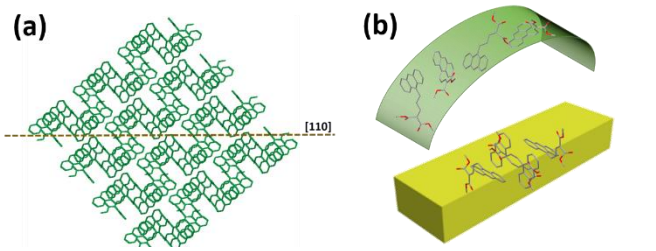

Figure 5. (a) Molecular arrangement of *cis*-**DMAAM** in the microblock showing separate layers along the (110) Miller plane (dashed line). (b) Schematic illustration showing the proposed photoinduced peeling process of *cis*-**DMAAM** microblock as the mixed *cis*/*trans* layer expands and detaches from the parent crystal. Hydrogen atoms are not shown for the sake of clarity.

To study the effect of pulse duration on the number of peels produced, a semi-quantitative experiment is performed on a sample of microblocks with 2.4 μm width. For sequential 1 s pulse durations, the block yields an average of 6 peels, each with an estimated thickness of ~400 nm. The peel thickness depends on the duration of the light exposure. For 1 s pulses on average 6 peels are observed. When the pulse duration is doubled to 2 s, 4 peels in total are liberated. When the pulse duration is extended to 5 s, roughly 2 peels are observed. Longer light pulses apparently increase the depth of photoreaction in the blocks and thus the thickness of the product layer that peels away. (Figure S10, Movie S6 and Tables S1-S3, ESI). The dynamics of the peeling also changes with pulse duration. For example, after a 1 s pulse, the peeling is complete after 10-20 s. After a 5 s pulse, the peeling process typically requires 60 s or longer (Movie S7-9, ESI). In all cases, the peeling occurred after the light is turned off, suggesting that a phase change or separation process is occurring as the molecules rearrange. If the microblocks are exposed to continuous irradiation, they undergo a continuous deformation without peeling (Movie S10).

In order to clarify the composition of the new phase that peeled off the parent block, a collection of *cis*-**DMAAM** microblocks was irradiated by sequential 1 s light pulses until they all peeled away to fragments. The peels were analyzed using HPLC and found to consist of 10-20% *trans*-**DMAAM** (Figure S11, ESI). This is consistent with our previous measurements on photoreacted nanowires and provides evidence that the photoisomerization does not proceed to 100% completion but instead reaches a photostationary state that contains a mixture of *cis* and *trans* isomers[24, 34]. The peeled photoproduct itself is not crystalline, as judged by its lack of any discernible x-ray or electron diffraction peaks, and lack of birefringence (Figure S12, ESI).

The delay between the initial light exposure and peeling may reflect the time required to form this new product phase by molecular migration within the block. The geometry of the peel also provides some clues as to its composition. The peel always curls inward, with the middle detaching first and the ends last. This bending curvature suggests that the outer surface of the peel is expanding, consistent with swelling due to loss of order and possibly solvent penetration. The clean detachment may be due to the unique faceting of the block crystal. As can be seen from

Figure 5a, the (110) Miller plane lies parallel to a 2-dimensional plane in the crystal that separates layers of *cis*-**DMAAM** molecules. These layers provide natural cleavage planes for layer detachment. The presence of SDS can facilitate this separation by penetrating along the incipient crack and further weakening the van der Waals attraction between **DMAAM** layers. The ability of SDS to modify the surface photoreactivity and induce amorphization in *trans*-**DMAAM** crystals has been shown previously.[41] The sequence of amorphization followed by delamination is shown schematically in Figure 5b.

In summary, this paper illustrates that it is possible to use surfactant mixtures and temperature to modify faceting during crystal growth and create well-defined microblocks of the photoisomerizable molecule *cis*-**DMAAM**. When these blocks are exposed to a pulse of 405 nm light, a novel peeling behavior is observed in which layers of uniform thickness detach from the parent block crystal. This peeling is caused by formation of a mixed *cis-trans* amorphous phase that grows in over time and expands to break away. The observation of sequential photoinduced peeling from a molecular crystal represents a new mode of photomechanical response. It can be thought of as a controlled fracture event that is reproducible thanks to the well-defined shape of the reactant crystals. These results illustrate how tuning crystal size and shape can lead to novel modes of photomechanical behavior.

C. J. Bardeen acknowledges support from the National Science Foundation, grant DMR-1810514. R. O. Al-Kaysi acknowledges the support of KSAU-HS/KAIMRC through grant RC10/104.

Conflicts of interest

In There are no conflicts to declare.

Notes and references

1. T. Kim, L. Zhu, R. O. Al-Kaysi and C. J. Bardeen, *ChemPhysChem*, 2014, **15**, 400-414.
2. J. M. Abendroth, O. S. Bushuyev, P. S. Weiss and C. J. Barrett, *ACS Nano*, 2015, **9**, 7746-7768.
3. T. J. White, ed., *Photomechanical Materials, Composites, and Systems*, 1 edn., Wiley, Hoboken, New Jersey, 2017.
4. T. Ikeda, J. Mamiya and Y. Yu, *Angew. Chem. Int. Ed.*, 2007, **46**, 506-528.
5. T. J. White, N. V. Tabiryan, S. V. Serak, U. A. Hrozhyk, V. P. Tondiglia, H. Koerner, R. A. Vaia and T. J. Bunning, *Soft Matter*, 2008, **4**, 1796-1798.
6. L. Liu, M.-H. Liu, L.-L. Deng, B.-P. Lin and H. Yang, *J. Am. Chem. Soc.*, 2017, **139**, 11333−11336.
7. R. O. Al-Kaysi and C. J. Bardeen, *Adv. Mater.*, 2007, **19**, 1276-1280.
8. L. Zhu, R. O. Al-Kaysi and C. J. Bardeen, *J. Am. Chem. Soc.*, 2011, **133**, 12569-12575.
9. L. Zhu, R. O. Al-Kaysi and C. J. Bardeen, *Angew. Chem. Int. Ed.*, 2016, **55**, 7073-7076.
10. S. Kobatake, S. Takami, H. Muto, T. Ishikawa and M. Irie, *Nature*, 2007, **446**, 778-781.
11. M. Morimoto and M. Irie, *J. Am. Chem. Soc.*, 2010, **132**, 14172-14178.
12.D. Kitagawa, H. Nishi and S. Kobatake, *Angew. Chem. Int. Ed.*, 2013, **52**, 9320-9322.
13. D. Kitagawa, R. Tanaka and S. Kobatake, *Phys. Chem. Chem. Phys.*, 2015, **17**, 27300--27305.
14. H. Koshima, N. Ojima and H. Uchimoto, *J. Am. Chem. Soc.*, 2009, **131**, 6890-6891.
15. H. Koshima, K. Takechi, H. Uchimoto, M. Shiro and D. Hashizume, *Chem. Commun.*, 2011, **47**, 11423-11425.
16. P. Naumov, J. Kowalik, K. M. Solntsev, A. Baldridge, J.-S. Moon, C. Kranz and L. M. Tolbert, *J. Am. Chem. Soc.*, 2010, **132**, 5845-5857.
17. N. K. Nath, L. Pejov, S. M. Nichols, C. Hu, N. Saleh, B. Kahr and P. Naumov, *J. Am. Chem. Soc.*, 2014, **136**, 2757-2766.
18. O. S. Bushuyev, A. Tomberg, T. Friscic and C. J. Barrett, *J. Am. Chem. Soc.*, 2013, **135**, 12556-12559.
19. H. Wang, P. Chen, Z. Wu, J. Zhao, J. Sun and R. Lu, *Angew. Chem. Int. Ed.*, 2017, **56**, 9463 –9467.
20. R. O. Al-Kaysi, A. M. Muller and C. J. Bardeen, *J. Am. Chem. Soc.*, 2006, **128**, 15938-15939.
21. D. K. Bucar and L. R. MacGillivray, *J. Am. Chem. Soc.*, 2007, **129**, 32-33.
22. A. E. Keating and M. A. Garcia-Garibay, in *Organic and Inorganic Photochemistry*, eds. V. Ramamurthy and K. S. Schanze, Dekker, New York, 1 edn., 1998, vol. 2, pp. 195-248.
23. R. Medishetty, A. Husain, Z. Bai, T. Runčevski, R. E. Dinnebier, P. Naumov and J. J. Vittal, *Angew. Chem. Int. Ed.*, 2014, **126**, 6017-6021.
24. R. Medishetty, S. C. Sahoo, C. E. Mulijanto, P. e. Naumov and J. J. Vittal, *Chem. Mater.*, 2015, **27**, 1821-1829.
25. E. Hatano, M. Morimoto, T. Imai, K. Hyodo, A. Fujimoto, R. Nishimura, A. Sekine, N. Yasuda, S. Yokojima and S. Nakamura, *Angew. Chem. Int. Ed.*, 2017, **56**, 12576-12580.
26. T. Kim, M. K. Al-Muhanna, S. D. Al-Suwaidan, R. O. Al-Kaysi and C. J. Bardeen, *Angew. Chem. Int. Ed.*, 2013, **52**, 6889-6893.
27. C. T. Sun and Z. H. Jin, *Fracture Mechanics*, Academic Press, Waltham, MA, 2012.
28. S. Saha, M. K. Mishra, C. M. Reddy and G. R. Desiraju, *Acc. Chem. Res.*, 2018, **51**, 2957-2967.
29. E. Ahmed, D. P. Karothu and P. Naumov, *Angew. Chem. Int. Ed.*, 2018, **57**, 837–8846.
30. H. Fu, D. Xiao, J. Yao and G. Yang, *Angew. Chem. Int. Ed.*, 2003, **42**, 2883-2886.
31. Y. Lei, Q. Liao, H. Fu and J. Yao, *J. Phys. Chem. C*, 2009, **113**, 10038-10043.
32. X. Zhang, X. Zhang, W. Shi, X. Meng, C. Lee and S. Lee, *J. Phys. Chem. B*, 2005, **109**, 18777-18780.
33. X. Zhang, C. Dong, J. A. Zapien, S. Ismathullakhan, Z. Kang, J. Jie, X. Zhang, J. C. Chang, C. S. Lee and S. T. Lee, *Angew. Chem. Int. Ed.*, 2009, **48**, 9121-9123.
34. Z.-Q. Lin, P.-J. Sun, Y.-Y. Tay, J. Liang, Y. Liu, N.-E. Shi, L.-H. Xie, M.-D. Yi, Y. Qian, Q.-L. Fan, H. Zhang, H. H. Hng, J. Ma, Q. Zhang and W. Huang, *ACS Nano*, 2012, **6**, 5309–5319.
35. S.-H. Yang, Z.-Q. Lin, N.-E. Shi, L.-Z. Jin, M.-N. Yu, L.-H. Xie, M.-D. Yia and W. Huang, *CrystEngComm*, 2015, **17**, 1448–1452.
36.L. Peng, Y.-N. Chen, Y. Q. Dong, C. He and H. Wang, *J. Mater. Chem. C*, 2017, **5**, 557-565.
37. R. O. Al-Kaysi, F. Tong, M. Al-Haidar, L. Zhu and C. J. Bardeen, *Chem. Commun.*, 2017, **53**, 2622-2625
38. F. Tong, W. Xu, M. Al-Haidar, D. Kitagawa, R. O. Al-Kaysi and C. J. Bardeen, *Angewandte Chemie*, 2018, **130**, 7198-7202.
39. M. B. Epstein and J. Ross, *J. Phys. Chem.*, 1957, **61**, 1578-1578.
40. M. S. Bakshi, *Cryst. Growth & Des.*, 2015, **16**, 1104-1133.
41. F. Tong, M. Liu, R. O. Al-Kaysi and C. J. Bardeen, *Langmuir*, 2018, **34**, 1627-1634.

Graphic Abstract

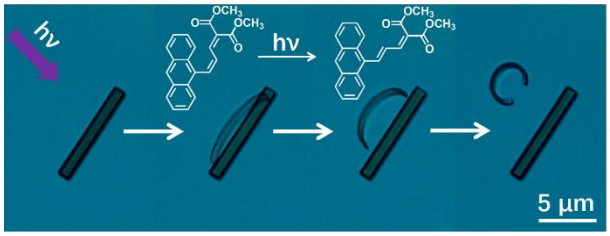

Photoisomerization of *cis*-dimethyl-2(3-(anthracen-9-yl)allylidene)malonate in a block-shaped microcrystal initiates a phase separation and delamination of the reacted layer from parent crystal.